Human dentin characteristics of patients with osteogenesis imperfecta: insights into collagen-based biomaterials

S Pragnère, J-C Auregan, C Bosser, A Linglart, M Bensidhoum, T Hoc, C Nouguier-Lehon, C Chaussain

Version of Record: https://www.sciencedirect.com/science/article/pii/S174270612030622X
Manuscript_f7906a5984bd469aad0269bdc00c7e87

Human dentin characteristics of patients with osteogenesis imperfecta: insights into collagen-based biomaterials

Pragnère S[a], Auregan J-C[b,c], Bosser C[a], Linglart A[d] Bensidhoum M[b], Hoc T[b,e], Nouguier-Lehon C[f], Chaussain C[g,h]

a Equipex IVTV, Centrale Innovation, 64 Chemin des Mouilles, 69130 Ecully, France
b Université de Paris, B3OA, UMR CNRS 7052, INSERM U1271, 10 Avenue de Verdun, 75010 Paris, France
c AP-HP, Antoine Béclère Université Paris-Saclay hospital, Orthopeadics Department, 157, rue de la Porte de Trivaux, 92140 Clamart, France
d Université de Paris Saclay, Le Kremlin-Bicêtre, France; AP-HP, Department of Endocrinology and Diabetology for children, Reference Center for Rare Disorders of the Calcium and Phosphate Metabolism, Filière OSCAR and Platform of expertise for rare diseases Paris-Sud, Bicêtre Paris-Saclay Hospital, Le Kremlin-Bicêtre, France,
e Mechanical Department, MSGMGC, Ecole Centrale de Lyon, 36 Avenue Guy de Collongue, 69134 Ecully Cedex, France
f Université de Lyon, LTDS UMR CNRS 5513, Ecole Centrale de Lyon, 36 Avenue Guy de Collongue, 69134 Ecully Cedex, France
g Université de Paris, Dental School, UR2496, Montrouge, F-92120, France
h AP-HP Reference Center for Rare Disorders of the Calcium and Phosphate Metabolism (OSCAR, ERN Bond), Dental Medicine Department, Bretonneau Hospital, GHN, 75018 Paris, France

Corresponding Author
Pr Thierry Hoc
Université de Paris,
B3OA Laboratory,
UMR CNRS 7052, INSERM U1271,
10 Avenue de Verdun,
75010 Paris, France
Email : thierry.hoc@inserm.fr

Abstract

Osteogenesis imperfecta (OI), also known as "brittle bone disease", is a rare genetic disorder of the skeleton, whose most benign form I corresponds to autosomal dominant mutations in the genes encoding type I collagen (*COLA1, COLA2*). Several associated skeletal manifestations are often observed but, surprisingly, while dentin defects often reflect genetic bone disorders, about half of OI patients have no obvious oral manifestations. Here, we investigated the collagen, mineral and mechanical properties of dentin from deciduous teeth collected from patients with mild form of OI and displaying no obvious clinical signs of dentinogenesis imperfecta. For the first time, an increase in the hardness of OI dentin associated with an increase in mineral content compared to healthy patients was reported. In addition, OI altered the tissue characteristics of the dentin-enamel junction but the interfacial gradient was preserved. The impact of changes in molecular structure due to mutations in OI was assessed by Raman microspectroscopy. Our results highlighted a change in the hydroxyproline-proline ratio in direct association with collagen mineralization. Our findings suggest that the evaluation of teeth could be an important aid for mild types of OI that are often difficult to diagnose clinically and provide experimental evidence that hydroxyproline content should be considered in future studies on collagen-based biomaterials.

Keywords: Deciduous teeth, biomineralization, Osteogenesis imperfecta, Hardness, Raman microspectroscopy.

1 Introduction

Osteogenesis imperfecta (OI), also known as « brittle bone disease », is a fairly common rare genetic skeletal disorder estimated to affect about 1/13,500–15,000 births [1,2].The best known classification of OI is given by Sillence, who divided OI cases into four types as early as 1979 [3]. In this classification, type I corresponds to the mildest form, type II to the perinatal lethal form, type III to the most severe form compatible with life, and type IV is an intermediate group. This classification covers 85-90% of OI patients and corresponds to autosomal dominant mutations in the genes encoding type I collagen (*COL1A1* and *COL1A2*). Although this classification is still widely used, several types have been added since 2006, when the first OI recessive gene was identified [4,5]. Over the last ten years, the Sillence classification, which was initially phenotypically based, now includes more than sixteen different types and this number is constantly increasing with new genes discovery [2]. Recently, Forlino *et al.* [6] proposed a classification into five groups based on the metabolic pathways compromised, especially those related to collagen formation, assembly and mineralization.

Consequently, there is a wide variety of clinical manifestations due to OI. Indeed, collagen is the most abundant protein in the human body and type I collagen is by far the predominant type found in connective tissue. The first clinical signs of OI are often the frequency of bone fractures in children, but at the bone-whole scale effects may include short stature and progressive skeletal deformities [7,8]. Several other manifestations such as blue sclera [9], dentinogenesis imperfecta [10–12], joint laxity [13], hearing loss [14], and often respiratory symptoms may be observed [15]. More details about the manifestations of OI and treatments based on orthopaedic surgery or bisphosphonates administration can be found in previous publications [16,17].

At microscopic scale, i.e. tissue scale, large majority of studies performed on OI human bones or OI murine models show an increased mineral content associated with a decreased organic matrix. The crystal size is smaller with a less well organized orientation [18–20], mechanical properties decreased [21] and more pronounced heterogeneity in collagen diameter fibrils is observed [22]. The discovery of numerous recessive OI mutations in various genes [2], such as *SERPINF1* [23,24], *CRTAP* [4,25,26], or *P3H1* encoding prolyl 3-hydroxylase 1 [27,28], has open new potential therapeutic targets. However, the knowledge about how these mutations impact the interactions between collagen fibres and hydroxyapatite crystals at the molecular scale is not fully understood.

Indeed, collagen biosynthesis and mineralization is probably one of the most complicated biological processes. The specific structure of the triple helix conformation of type I fibrillar collagen is characterized by a repeating motif X-Y-Gly amino sequence, with glycine (Gly) in third position being a requirement and the most abundant residues at the X and Y sites being proline (Pro) and hydroxyproline (Hyp), respectively [29]. In the Pro-Hyp-Gly motif, hydroxyproline is usually in second position allowing the stabilization of the triple helix but many studies are working on several defective genes involved in the stabilization process. Over the last decade, numerous studies have been carried out on the collagen mechanical properties at the nanoscale, analysing in particular the behaviour of fibrils and fibril-fibril interactions [30–33]. Knowledge of behaviour at the nanoscale is particularly relevant for OI, where glycine substitution in the triple helix is known to be one of the

most common mutations whose clinical forms are classically observed [34,35]. Molecular or coarse grain simulations [36–40] of glycine substitution have shown that the mechanical behaviour of collagen fibrils is strongly modified and that a single point mutation leading to a helical perturbation affects several length scales. Similarly, the most common post-translational modification of proline in hydroxyproline has recently been studied at the nanoscale using molecular dynamics simulations [41], showing that proline-rich collagens have higher stiffness and Young's modulus than hydroxyproline-rich collagens.

All these studies point out the spectacular advances in the understanding of this rare disorder. However, while techniques are now mature to access mechanical properties, crystal quality or post-translational modification of tissues [42], data on human tissues in the literature remain weak. In addition, human samples are often bone fragments obtained during orthopaedic bone alignment surgery, often treated with bisphosphonates that can cause modifications [43]. Due to its accessibility, several studies [12, 44] have been performed on dentin from teeth with or without OI, revealing microstructural and mechanical changes. However, these results need to be reinforced, in particular on deciduous teeth that have been mineralized prior to initiation of bisphosphonate treatment.

The major oral manifestation of OI is altered dentin formation (dentinogenesis imperfecta), manifesting by discoloration of the dentition, brittle teeth prone to early and severe attrition, bulbous crowns and early obliteration of the pulp in both dentitions [45]. Dentin is very similar to bone in terms of the composition of the extracellular matrix, which is secreted by odontoblasts and osteoblasts, respectively. Hence, dentin consists of a mainly type I collagen organic matrix embedded in hydroxyapatite crystals [46]. However, unlike bone, dentin is not remodelled and is not involved in the regulation of the calcium and phosphate metabolism. Surprisingly, while dentin defects reflect genetic disorders affecting bone mineralisation [45], about one half of the patients with OI show no obvious oral manifestations. Here, we raise the hypothesis that OI patients without oral manifestations still display a modification of dentin (subclinical dentinogenesis imperfecta), in terms of collagen, minerals and mechanical properties and that the investigation of these defects may aid in the diagnosis of mild osteogenesis imperfecta.

2 Materials and methods

2.1 Samples and preparation

Teeth were extracted from control individuals and patients with OI. None of the donors included in the present study had clinical signs of dentinogenesis imperfecta. The OI group consisted of six deciduous teeth from four patients with mild type OI. The control group consisted of eight deciduous teeth from six healthy donors of the same sex and age. Clinical data about the OI patients are provided in Table 1. All the teeth were acquired with the informed consent of the patients and parents, in accordance with the ethical guidelines laid down by French law (agreement IRB 00006477 and n° DC-2009-927, Cellule Bioéthique DGRI/A5). The whole teeth were gently cleaned with tap water and stored dry at -20°C until their analysis. For each sample, buccolingual sections 3 mm thick in the centre of the tooth were prepared as follows. The specimens were polished on sandpaper (#1200) to obtain plano-parallel surfaces, then polished with 1-µm diamond powder and rinsed in an ultrasonic bath. The diagnostic criterion of DI was performed using radiology and optical images.

Representative optical images of dentin from OI sample without DI, DI sample and control sample are given in supplementary materials (Supplemental Figure). For each sample, as soon as the surface preparation was completed, the samples were directly analyzed by nanoindentation followed immediately by Raman microspectroscopy acquisitions.

Patient number	Form	Phenotype	Bisphos-phonate treatment	Gender	Age (y)	Teeth
1	Sporadic	Mild OI (type IV)	Onset at 16 months	M	9	2 deciduous molars
2	Familial	Mild OI (type I)	From 2.5 to 4.5 years/old	F	11	2 deciduous canines
3	Familial	Mild OI (type I)	Onset at 24 months	M	10	1 deciduous molar
4	Familial	Mild OI (type I)	Onset at 13 year/old	M	12	1 deciduous canine

Table 1: Clinical characteristics of the patients with OI.

2.2 Nanoindentation

The mechanical properties of the dentin were obtained using a commercial nanoindenter (Agilent Nanoindenter G200, ScienTec, Les Ulis, France) following previously published protocols [20,47]. Fused silica was used to calibrate the contact surface of the Berkovich diamond tip. Two zones of interest were defined within the dentin (Figure 1): an outer zone near the dentin-enamel junction (DEJ) and a middle zone in the centre of the dentin, referred to External (Ext) and Middle (Mid) in the following of the study, respectively. Six measurement points were taken in each area of the sample. The location of each indentation was manually set on a line parallel to the DEJ in the outer areas and on a grid of points in the middle area. A minimum spacing of 200 µm between each point was imposed. A conventional constant strain rate of 0.05 s^{-1} and a maximum depth of 2µm were used. The material was assumed to be linear, elastic and isotropic and the classical Oliver and Pharr method was used in the study [48]. The Poisson's ratio was assumed to be 0.3 [49,50]. Young's modulus and contact hardness for each indentation point was averaged over the 800-1800 nm depth plateau obtained from continuous stiffness measurement (CSM).

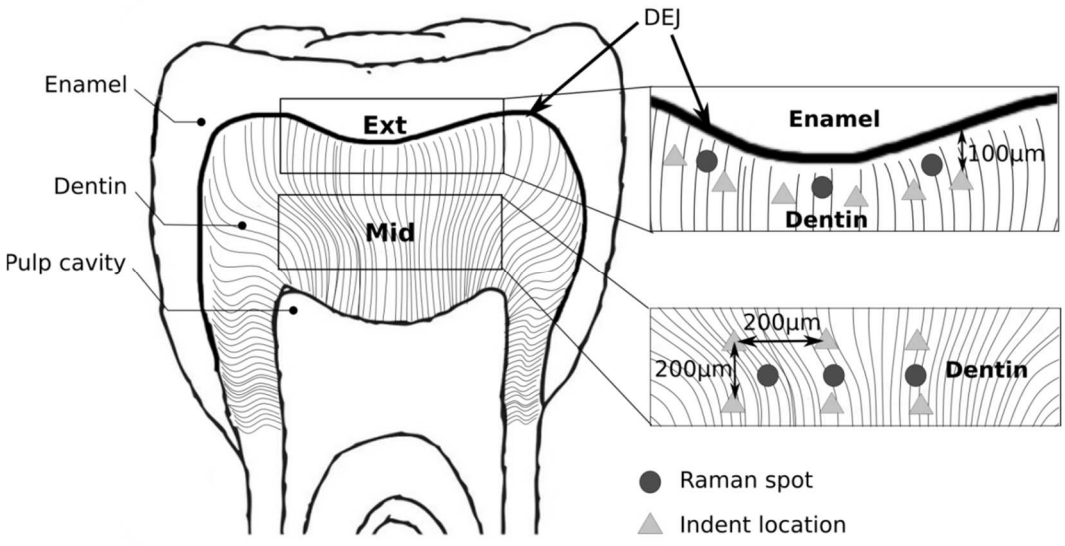

Figure 1: Diagram showing the localization of indents within the two zones of interest in the dentin: external (Ext), near the dentino-enamel junction (DEJ), and middle (Mid). Six indents (triangle markers) and three Raman spectra (circle markers) have been run in each zone.

2.3 Raman microspectroscopy

Raman spectroscopy (LabRAM HR 800, Horiba Jobin Yvon, Villeneuve d'Ascq, France) was performed on the same sample surface as that used for nanoindentation according to a previously published protocol [20]. This technique uses Raman diffusion (inelastic) to obtain information on the composition of the material. A monochromatic laser is used to excite the molecules in the sample. The difference between the energy of the incident and emitted light produces a spectrum that provides information about the molecules present within the sample[51].

Figure 2 shows a typical spectrum for a control tooth. A 785 nm laser was used to excite the molecule in the material. The 50x objective and 0.75 numerical aperture produced a laser spot approximately 2 µm in diameter on the sample. Acquisitions were made over the spectral range from 350 cm^{-1} to 1750 cm^{-1}, with an integration time of 60 s and one accumulation. Four spectra were acquired for each point, and 3 points in each area close to the nanoindentation points were measured for each of the samples. The Raman spectra were acquired at a point below the surface where the intensity of the phosphate peak at 961 cm^{-1} was maximum. LabSpec software (Horiba Jobin Yvon, Villeneuve d'Ascq, France) was used to despike the spectra. A custom Matlab routine (version R2016a, MathWorks, Natick, MA, USA) was applied on each of the four spectra per point to subtract background. The four spectra were then averaged and deconvolution was performed to compute peak intensity and position of the band of interest.

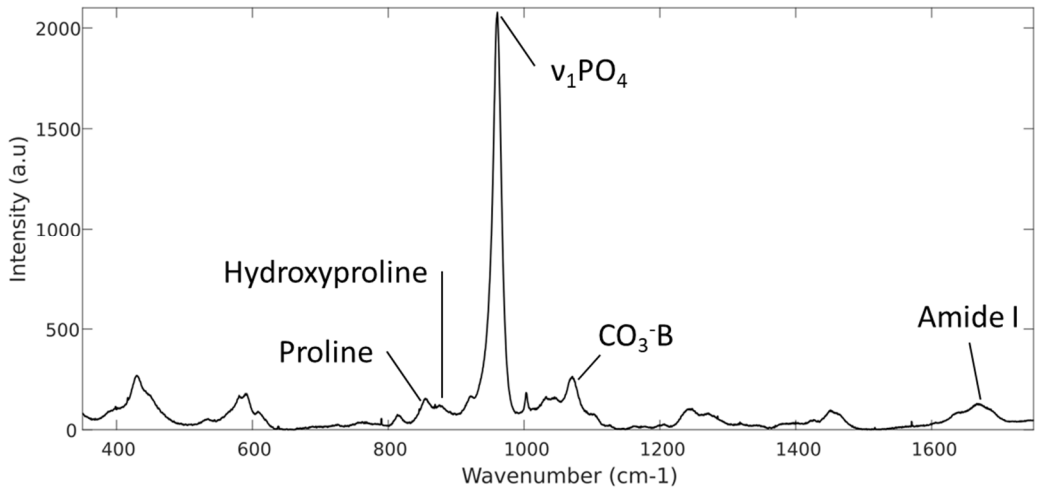

Figure 2: Typical Raman spectra for a control dentin obtained after background substraction, averaging of the 4 spectra and smoothing. The peak at 961 cm^{-1} corresponds to phosphate, the peak at 1075 cm^{-1} corresponds to carbonate, the peak at 853cm^{-1} corresponds to proline, the peak at 875cm^{-1} corresponds to hydroxyproline and the peak at 1667 cm^{-1} corresponds to Amide I.

Four maximum intensity ratios were calculated from the spectra (Figure 2), i) the mineral-to-matrix ratio (MMR), describing the mineral content compared to the collagen matrix, was calculated in two different ways : the ratio between the maximum intensities of ν_1PO_4 (961 cm^{-1}) and Amide I (1667 cm-^{1}), referred to as MMR Amide I, and the ratio between the maximum intensities of ν_1PO_4 (961 cm^{-1}) and Proline (853 cm^{-1}), referred to as MMR Proline, in the following of the study ; ii) the carbonate-to-phosphate ratio, as the ratio between CO_3-B (1075 cm^{-1}) and ν_1PO_4 (961 cm^{-1}), which indicates the rate of substitution of phosphate by carbonate in the B-mode; and iii) the hydroxyproline-to-proline ratio (875 cm^{-1} to 853 cm^{-1}) which reflects the post-translational modifications of the collagen obtained by deconvolution process [42]. The deconvolution parameters were identical for OI group and control group. Crystallinity, which corresponds to the inverse of the full width at half the ν_1PO_4 peak (961 cm^{-1}), and the wavenumber shift of the hydroxyproline band were also studied [52,53].

2.4 Statistical analysis

Statistical analysis was performed using R software (R Foundation for Statistical Computing, Vienna, Austria). Mann-Whitney tests were used to assess the significant differences between mechanical properties and biochemical composition of the control (n=8) and OI (n=6) groups. To assess the effect of the zone, mechanical and biochemical values of the external and middle zones were compared by Wilcoxon test for paired samples. The level of significance for all analyses corresponded to an α-risk of 5%. p-values were corrected for multiple comparisons by the Benjamini-Hochberg method. Linear correlations between hardness and mineral-to-matrix ratio or between hydroxyproline-to-proline ratio and mineral-to-matrix ratio were evaluated by Spearman's correlation test.

3 Results

3.1 Mechanical properties

From a mechanical point of view, we analyzed two parameters: hardness and Young's modulus. Particular attention was paid to the hardness of this brittle material which is related to the yield strength and the occurrence of fractures. Figure 3 shows the average hardness measured by nanoindentation in the external and middle zone for the control and OI groups. The mean (S.D) values of the hardness in the external zone were 0.76 (0.05) GPa and 0.98 (0.08) GPa for the control and OI groups, respectively. In the middle zone, the mean hardness values (S.D) for the control and OI groups were 0.84 (0.05) GPa and 1.08 (0.04) GPa, respectively. The mean hardness was then significantly lower for both external zone and middle zone ($p = 7\ 10^{-4}$ and $p = 1\ 10^{-3}$, respectively) for the control group than for the OI group.

Young's modulus showed similar trends with significantly lower values in the control group than in the OI group (data not shown).

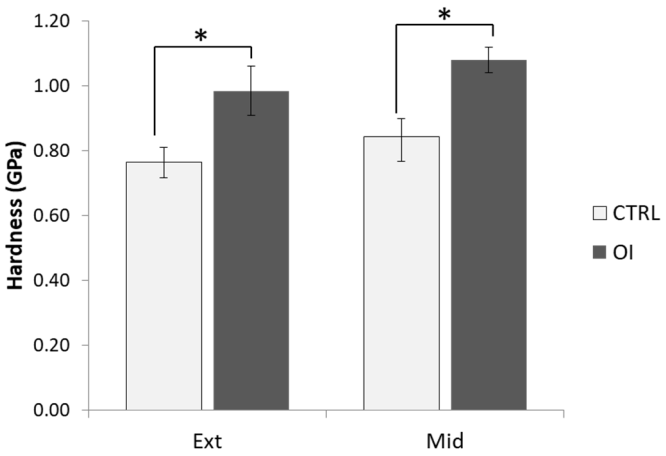

Figure 3: Mean hardness for control (CTRL) and OI groups. Mean hardness is higher in the OI group than in the control group regardless of the zone. Error bars represent standard deviation. * p-value <0.05 between control and OI group.

3.2 Collagen and mineral properties

The different data measured by Raman microspectroscopy and described earlier in the paragraph "Material and methods" are given in figure 4 for the OI and control groups, measured in the middle and external areas.

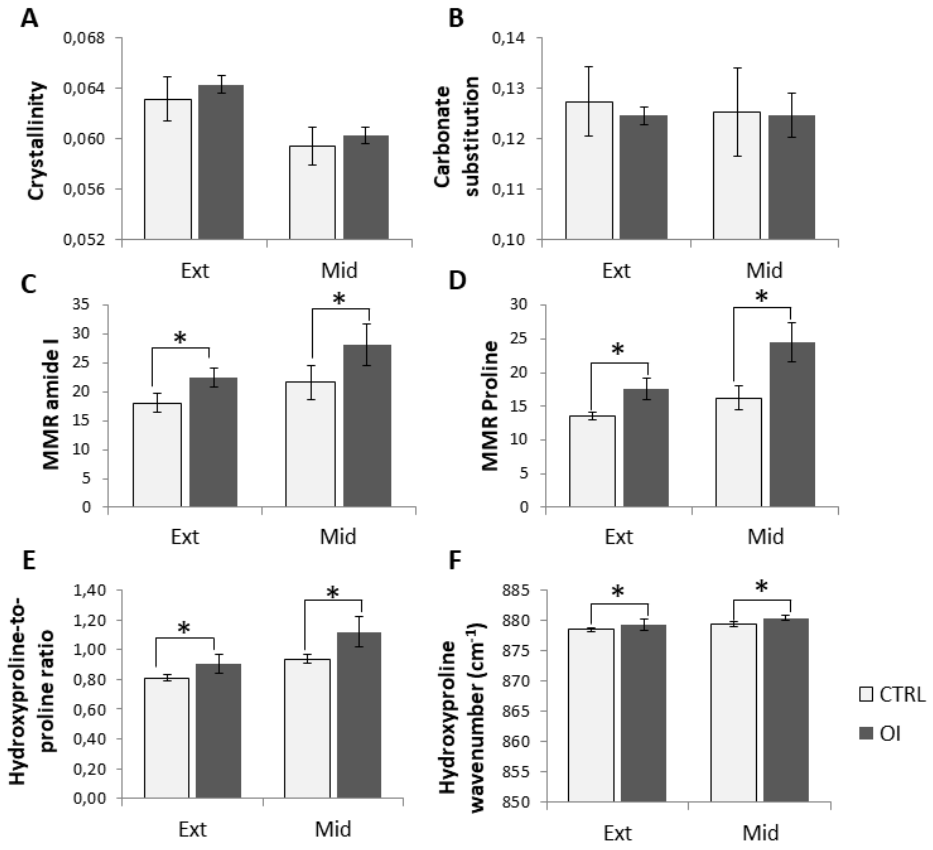

Figure 4: : Barplot illustrating (A) crystallinity, (B) carbonate substitution, (C) mineral-to-matrix ratio (MMR Amide I), (D) mineral-to-matrix ratio (MMR Proline), (E) hydroxyproline-to-proline ratio and (F) Hydroxyproline wavenumber, for control (CTRL) and OI group. Mean MMR and hydroxyproline-to-proline ratio are higher in the OI group than in the control group regardless of the zone. Error bars represent standard deviation. * p-value<0.05 between control and OI group.

Figures A and B show the quality of the mineral through analysis of crystallinity and carbonate substitution rate, respectively. There was a trend of higher crystallinity from 0.059 (0.001) to 0.060 (0.001) (from 0.063 (0.002) to 0.064 (0.001), respectively) and a lower carbonate substitution rate from 0.125 (0.009) to 0.125 (0.004) (from 0.127 (0.007) to 0.125 (0.002), respectively) for the OI dentin samples in the middle zone (in the external zone, respectively)

The mean (S.D.) values of the mineral-to-matrix ratio (MMR Amide I) in the external zone, for the control and OI groups were 18.07 (1.64) and 22.43 (1.68), respectively (Figure 4C). The mean (S.D.) values of the mineral-to-matrix ratio in the middle zone for the control and OI groups were 28.13 (3.71) and 21.68 (2.92), respectively. The mineral-to-matrix ratio was significantly higher ($p = 7\ 10^{-4}$) in the external zone ($p= 5\ 10^{-3}$ in the middle zone, respectively) for the OI group than for the control group.

The mean (S.D.) values of the mineral-to-matrix ratio (MMR Proline) in the external zone for the control and OI groups were 13.51 (0.58) and 17.59 (1.52), respectively (Figure 4D). The mean (S.D.) values of the mineral-to-matrix ratio in the middle zone for control and OI groups were 16.26 (1.70) and 24.5 (2.98), respectively. The mineral-to-matrix ratio was significantly higher ($p = 7\ 10^{-4}$) in the external zone ($p= 1\ 10^{-3}$ in the middle zone, respectively) for the OI group than for the control group.

The same results were obtained on hydroxyproline-to-proline ratio, given on figure 4E. The mean (S.D.) values of the hydroxyproline-to-proline ratio in the external zone for the control and OI groups were 0.81 (0.02) and 0.91 (0.07), respectively. The mean (S.D.) values of the hydroxyproline-to-proline ratio in the middle zone for the control and OI groups were 0.94 (0.03) and 1.12 (0.10), respectively. The hydroxyproline-to-proline ratio was significantly higher ($p = 4\ 10^{-3}$) in the external zone ($p= 1\ 10^{-3}$ in the middle zone, respectively) for the OI group than for the control group.

The mean (S.D.) values of the hydroxyproline band wavenumber in the external for the control and OI groups were 878.53 (0.29) cm^{-1} and 879.30 (1.00) cm^{-1}, respectively (Figure 4F). The mean (S.D.) values of the of the hydroxyproline band wavenumber in the middle zone for control and OI groups were 879.37 (0.48) cm^{-1} and 880.43 (0.45) cm^{-1}, respectively. The positive shift in hydroxyproline band wavenumber for the OI group was significant ($p = 3\ 10^{-2}$) in the external zone ($p = 2\ 10^{-3}$ in the middle zone, respectively) compared to the control group.

Finally, for both the control and OI groups, the crystallinity values measured in the middle zone were lower compared to external zone while the MMR Proline values, the MMR Amide I values and the hydroxyproline-to-proline ratio values measured in the middle zone were greater compared to the external zone. A positive shift in hydroxyproline band wavenumber between the external and middle zones was also recorded.

3.3 Hydroxyproline-to-proline ratio analysis

To highlight the difference in hydroxyproline-to-proline ratio all Raman spectra in the 800-900cm^{-1} range, including hydroxyproline and proline peaks, are given in Figure 5A in the middle zone. A strong difference was observed between the control spectra, in light grey, and the OI spectra, dotted line in dark grey. In particular, all control spectra were higher than the OI spectra. In terms of relative intensity, for each spectrum, the difference between the proline peak at 853 cm^{-1} and the hydroxyproline peak at 875 cm^{-1} was less pronounced in the OI group than in the control group. The effect of pathology on the hydroxyproline-to-proline ratio is clearly revealed by the average of all the OI and control spectra (Figure 5B) which shows the tightness between the proline and hydroxyproline intensity peaks in the OI group.

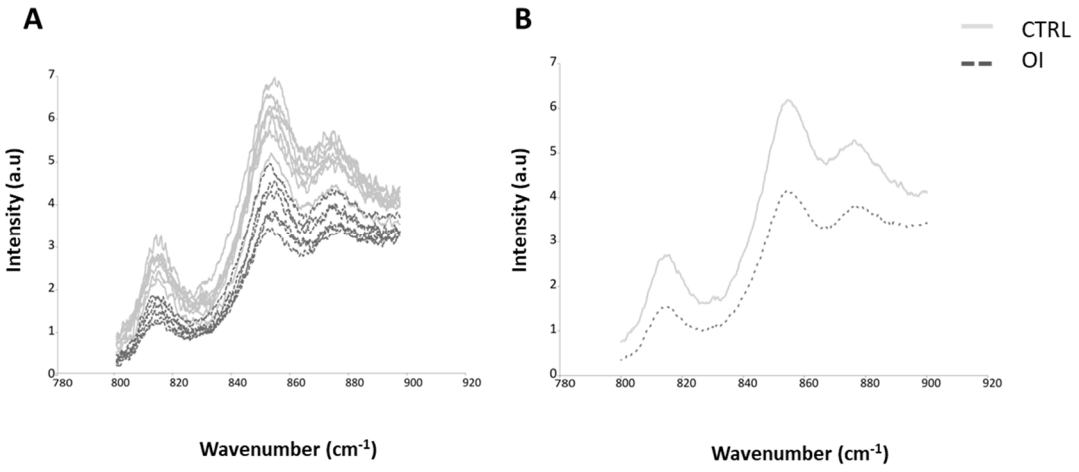

Figure 5: Raman spectra of the range 800-900cm^{-1} show that the hydroxyproline-to-proline ratio is higher in the OI group than in the control group. A: Spectra in the range 800-900cm^{-1} of all the teeth in the middle zone (OI and control group). B: Average spectra of OI and control group in the range 800-900cm^{-1} for the middle zone.

3.4 Correlations between mineral to matrix ratios and mechanical properties

Linear correlations between hardness and mineral to matrix ratio (MMR Amide I and MMR Proline) values, measured for all individuals in several areas, were investigated. For external zone (respectively middle zone), these parameters are linearly correlated with a reasonably high correlation coefficient; r = 0.84, p = 1.5 10^{-4} for MMR Proline and r = 0.7, p = 5 10^{-3} for MMR Amide I (respectively, r = 0.83, p = 2.8 10^{-4} for MMR Proline and r = 0.64, p = 1 10^{-2} for MMR Amide I). Figure 6 also shows a reasonably high correlation coefficient; r = 0.70, p = 6 10^{-5} for MMR Amide I and r = 0.84, p = 1 10^{-6} for MMR Proline, when considering all measurements. This result indicates that an increase in mineral to matrix ratios leads to an increase in hardness, regardless of the individuals and zones (OI, control, external and middle zone).

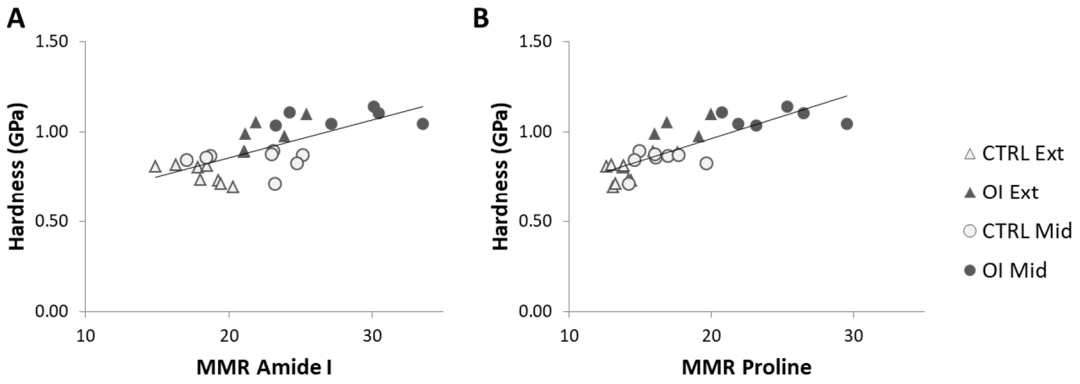

Figure 6: Linear correlation between mineral-to-matrix ratio (MMR) and hardness (H). A: MMR Amide I and hardness. B: MMR Proline and hardness.

3.5 Correlations between mineral to matrix ratios and hydroxyproline-to-proline ratio

The linear correlations between the values of mineral to matrix ratio (MMR Amide I and MMR Proline) and hydroxyproline-to-proline ratio were examined for the OI and control individuals (Figure 7). These parameters clearly correlate linearly with a reasonably high correlation coefficient (r =0.82 p =10^{-6} for MMR Amide I, r = 0.85, p = 10^{-6} for MMR Proline). This result indicates a positive relationship between the mineral-to-matrix ratio and the hydroxyproline-to-proline ratio, whatever individuals and areas (OI, Control, External and Middle).

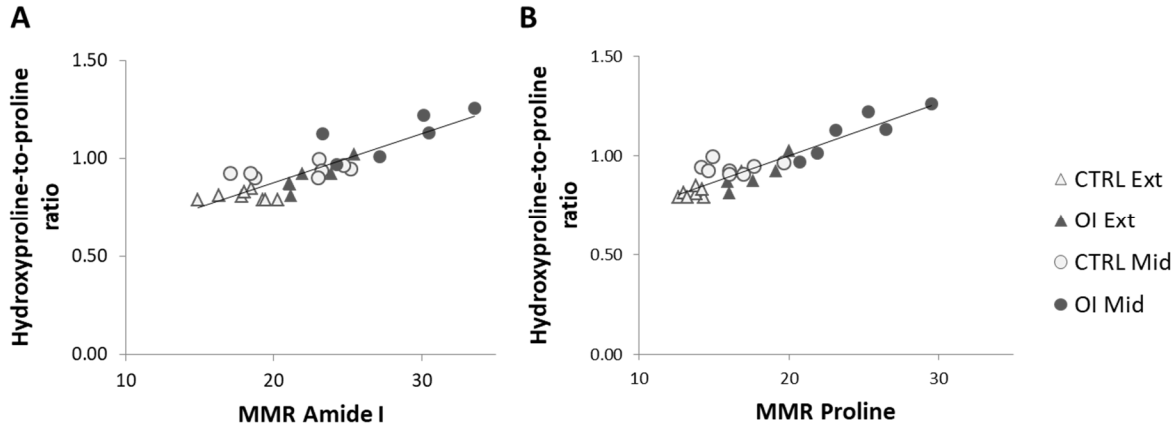

Figure 7: Linear correlation between mineral-to-matrix ratio (MMR) and hydroxyproline-to-proline ratio. A: MMR Amide I and hydroxyproline-to-proline ratio. B: MMR Proline and hydroxyproline-to-proline ratio.

4 Discussion and conclusions

The mechanical properties, especially hardness, of healthy human dentin are well known in the literature [50,54–57]. In the present study, the results are in good agreement with these data with a mean value of dentin hardness in the middle zone close to 1 (0.98 +/-0.08) GPa. In addition, many studies focus on the specific properties of DEJ. A decrease in hardness and an increase in crystallinity of dentin close to DEJ compared to the middle zone are reported [58–60]. In this study, a decrease in hardness close to 9% and an increase in crystallinity close to 6% in the near DEJ zone compared to the middle zone were also observed. Surprisingly, while one half of OI patients have no obvious clinical manifestations of dentinogenesis imperfecta (DI) [11,45], to date and to our knowledge, no human dentin studies have been carried out on OI patients without clinical manifestations of DI. As a result, the only studies available in the literature focus on patients with DI and show lower dentin hardness than healthy ones [12,61,62].

To the best of our knowledge, the present study is the first study reporting an increase in dentin hardness in patients with osteogenesis imperfecta without clinical manifestations of DI. In the literature, the only relevant study was carried out by Lopez *et al.* [63] on a mouse model of the Col1a2^{oim} mutation displaying also an increase in dentin hardness. The small number of samples and the size of the murine teeth involved in this study made the difference in dentin hardness near and far from the DEJ difficult to assess. In the present study, this spatial difference in hardness of OI dentin was measured and, as in healthy patients, there was a decrease in dentin hardness close to 9% in the area close to DEJ compared to the value measured in the middle area. It is important to note that whatever the healthy or diseased tooth, the spatial gradient of the mechanical properties of dentin is the same, with a decrease in dentin hardness value near the dentin/enamel interface.

The increase in hardness of OI dentin suggests an increase in mineral content. To confirm this hypothesis, the mineral to matrix ratios (MMR), which express the amount of minerals on amount of collagen, were measured by Raman microspectroscopy. The MMR was derived from Amide I and Proline peaks to ensure that the relative increase in mineral content is independent of the selected organic band [51,64–66]. As expected, MMR Raman ratios were higher in OI patients than in healthy patients, independently of the study area. More surprisingly, the mineral quality (crystallinity, maturation) was not affected by the pathology, unlike that found in bone tissue [18,20]. Therefore, a direct linear relationship between dentin hardness and MMR value is obtained for any tooth studied. It should be noted that the best correlation is obtained with the MMR calculated with the proline peak, which was previously reported by Bi *et al.* [25,67] in a mouse model of the Col1a2^{oim} mutation. The decrease in the amount of collagen classically observed in OI pathology [18] could explain the increase in the MMR ratio but not the increase in dentin hardness. Consequently, OI dentin contains a greater number of not significantly altered crystals leading to higher hardness.

Unfortunately, the interaction between mineral and collagen is still a subject of debate despite the great progress made over the last decade. Indeed, the process of biomineralization in bones and teeth is difficult to understand because of the complex hierarchic structure of collagen. It is now widely accepted that the crystal is present inside the collagen fibrils: in the "gap region", in the "intermolecular distance" but also in the extrafibrillar zone [30,31]. The mineral crystals themselves

form an interconnected mineral network with a helical morphology that could be shaped by the collagen network [68]. At nanoscale, molecular simulations also showed that changing the characteristic lengths scale of the collagen molecule has a direct effect on the deformation mechanisms and that even a small increase in the mineral density increases the mechanical properties of this complex network [33,69]. In the case of osteogenesis imperfecta, destabilization of the triple helix structure due to glycine substitution leads to changes in the structure of the molecules, including kink, local unfolding in the vicinity of the mutation, or an increase in intermolecular spacing. This new molecule conformation modifies the characteristic lengths scale increasing flexibility and reducing stiffness of collagen fibril [36–40]. These models show also that a single point mutation could lead to a dramatic reduction in mechanical strength of mineralized OI tissue at macroscopic scale.

In the present study, we hypothesize that defects in collagen synthesis, structure or transformation should be reflected in the hydroxyproline to proline, which is classically involved in the stabilization of the collagen triple helix. Raman microspectroscopy provides both the ratio of proline to hydroxyproline and the displacement of their respective Raman bands. To date and to the best of our knowledge, this is the first study in which the hydroxyproline-to-proline ratio and wavenumber of the hydroxyproline band in the OI group were reported to be increased compared to the control group. This result is obtained irrespective of the dentin area studied.

Recently, molecular dynamics simulations by Ghanaeian *et al.* [41] revealed that hydroxyproline rich collagens have lower stiffness and Young's modulus than proline-rich collagens. The increase in the hydroxyproline-to-proline ratio reported in the present study for the OI group should therefore correspond to a decrease in the stiffness and an increase in the elasticity of collagen, which is consistent with the properties of OI collagen fibrils described above. In addition, an increase in hydroxyproline is also consistent with higher mineralization, as demonstrated by Toworfe *et al.* [70] where hydroxylated surfaces enhanced calcium phosphate nucleation, or Buckley *et al.* [71] reporting Raman microspectroscopy of hydroxyproline-to-proline ratio obtained on different tissue and computational evidence that hydroxyproline is energetically the most favourable [72].

With respect to the wavenumber shift of the hydroxyproline band, several studies have been carried out on the sensitivity of hydroxyproline bands during the stretching of a collagen fibre [52,73,74]. While no significant difference is observed on collagen for low deformation values, this shift in the wavenumber of the hydroxyproline band appears for mineralized fibers at an early stage of deformation and this effect is enhanced as mineralization increases. Although studies have not yet been able to fully understand the molecular mechanisms behind this phenomenon, the shift observed by Raman microspectroscopy seems to reflect the quality of the interface between the mineral and the tropocollagen. It can therefore be hypothesized that the shift of the hydroxyproline band observed in our study between the OI group and the control group could be related to incompetence of collagen matrix mineralization.

This study obviously has several limitations. The first is the choice of samples analyzed. The experiments were conducted only on deciduous teeth. Noteworthy, the deciduous tooth is a convenient sample to study as it is easily available due to the natural shedding of teeth [45]. In addition, primary teeth mainly form before and around birth and mineralize therefore before the onset of treatments such as bisphosphonates which accumulate within mineralized tissues. However,

the present study should be reproduced on permanent teeth in order to consolidate the results. Similarly, we focused on a population of mild OI. It would also be interesting to consolidate this study on more severe cases of OI. And it is obvious that an experimental campaign conduct on bone samples including remodeling process is necessary in a future work. The second limitation arose in the light of our results which show a deficient mineralization of the collagen matrix. A more detailed analysis of the mineral with regard to the spatial distribution and orientation of crystals in dentin at the nanoscale, [28], could have highlighted some mechanisms. Along this line, several posttranslational modifications, such as hydroxylation of specific lysine residues, glycosylation of specific hydroxylysine residues, or formation of crosslinking were not directly investigated in the present study.

To our knowledge, this is the first study of human dentin in OI patients without clinical manifestations of DI. This study provides experimental evidence that changes in molecular structure due to mutations in OI can be assessed by Raman microspectroscopy and may shed further light on the molecular mechanisms obtained in future molecular simulations. Our data show an increase in dentin hardness and in hydroxyproline content, which both affect collagen mineralization in OI teeth. Interestingly, the spatial gradient of the mechanical properties of dentin is preserved in OI. Our findings reinforce our hypothesis that proline and hydroxyproline content should be taken into account in future studies on collagen-based biomaterials. Further research is needed to explore the underlying mechanisms at molecular scales leading to a modification in hydroxyproline-to-proline ratio in regard of collagen mineralization. In addition, deciduous tooth evaluation could be an important aid for the mild types of OI that are often difficult to diagnose clinically.

5 Acknowledgments

We would like to thank the IVTV ANR-10-EQPX-06-01 for its financial support, and the members of the French Association Osteogenesis Imperfecta (AOI) for their valuable discussions. Authors thanks Dr Fernando Ramirez Rozzi (MNHN, CNRS, Université de Paris, France) for helpful discussion regarding dentin tubular organization.

6 References

[1] K. Lindahl, E. Åström, C.-J. Rubin, G. Grigelioniene, B. Malmgren, Ö. Ljunggren, A. Kindmark, Genetic epidemiology, prevalence, and genotype–phenotype correlations in the Swedish population with osteogenesis imperfecta, Eur. J. Hum. Genet. 23 (2015) 1042–1050. https://doi.org/10.1038/ejhg.2015.81.

[2] G.R. Mortier, D.H. Cohn, V. Cormier-Daire, C. Hall, D. Krakow, S. Mundlos, G. Nishimura, S. Robertson, L. Sangiorgi, R. Savarirayan, D. Sillence, A. Superti-Furga, S. Unger, M.L. Warman, Nosology and classification of genetic skeletal disorders: 2019 revision, Am. J. Med. Genet. A. 179 (2019) 2393–2419. https://doi.org/10.1002/ajmg.a.61366.

[3] D.O. Sillence, A. Senn, D.M. Danks, Genetic heterogeneity in osteogenesis imperfecta., J. Med. Genet. 16 (1979) 101–116. https://doi.org/10.1136/jmg.16.2.101.

[4] A.M. Barnes, W. Chang, R. Morello, W.A. Cabral, M. Weis, D.R. Eyre, S. Leikin, E. Makareeva, N. Kuznetsova, T.E. Uveges, A. Ashok, A.W. Flor, J.J. Mulvihill, P.L. Wilson, U.T. Sundaram, B. Lee, J.C. Marini, Deficiency of cartilage-associated protein in recessive lethal osteogenesis imperfecta, N. Engl. J. Med. 355 (2006) 2757–2764. https://doi.org/10.1056/NEJMoa063804.

[5] R. Morello, T.K. Bertin, Y. Chen, J. Hicks, L. Tonachini, M. Monticone, P. Castagnola, F. Rauch, F.H. Glorieux, J. Vranka, H.P. Bächinger, J.M. Pace, U. Schwarze, P.H. Byers, M. Weis, R.J.

Fernandes, D.R. Eyre, Z. Yao, B.F. Boyce, B. Lee, CRTAP Is Required for Prolyl 3- Hydroxylation and Mutations Cause Recessive Osteogenesis Imperfecta, Cell. 127 (2006) 291–304. https://doi.org/10.1016/j.cell.2006.08.039.
[6] A. Forlino, J.C. Marini, Osteogenesis imperfecta, The Lancet. 387 (2016) 1657–1671. https://doi.org/10.1016/S0140-6736(15)00728-X.
[7] F.H. Glorieux, Osteogenesis imperfecta, Best Pract. Res. Clin. Rheumatol. 22 (2008) 85–100. https://doi.org/10.1016/j.berh.2007.12.012.
[8] U.E. Pazzaglia, T. Congiu, P.C. Brunelli, L. Magnano, A. Benetti, The Long Bone Deformity of Osteogenesis Imperfecta III: Analysis of Structural Changes Carried Out with Scanning Electron Microscopic Morphometry, Calcif. Tissue Int. 93 (2013) 453–461. https://doi.org/10.1007/s00223-013-9771-1.
[9] D. Sillence, B. Butler, M. Latham, K. Barlow, Natural history of blue sclerae in osteogenesis imperfecta, Am. J. Med. Genet. 45 (1993) 183–186. https://doi.org/10.1002/ajmg.1320450207.
[10] M.J. Barron, S.T. McDonnell, I. MacKie, M.J. Dixon, Hereditary dentine disorders: dentinogenesis imperfecta and dentine dysplasia, Orphanet J. Rare Dis. 3 (2008) 31. https://doi.org/10.1186/1750-1172-3-31.
[11] M. Biria, F.M. Abbas, S. Mozaffar, R. Ahmadi, Dentinogenesis imperfecta associated with osteogenesis imperfecta, Dent. Res. J. 9 (2012) 489–494.
[12] S. Ibrahim, A.P. Strange, S. Aguayo, A. Shinawi, N. Harith, N. Mohamed-Ibrahim, S. Siddiqui, S. Parekh, L. Bozec, Phenotypic Properties of Collagen in Dentinogenesis Imperfecta Associated with Osteogenesis Imperfecta, Int. J. Nanomedicine. 14 (2019) 9423–9435. https://doi.org/10.2147/IJN.S217420.
[13] F.E. McKiernan, Musculoskeletal manifestations of mild osteogenesis imperfecta in the adult, Osteoporos. Int. 16 (2005) 1698–1702. https://doi.org/10.1007/s00198-005-1905-5.
[14] F.K. Swinnen, P.J. Coucke, A.M. De Paepe, S. Symoens, F. Malfait, F.V. Gentile, L. Sangiorgi, P. D'Eufemia, M. Celli, T.J. Garretsen, C.W. Cremers, I.J. Dhooge, E.M. De Leenheer, Osteogenesis imperfecta: the audiological phenotype lacks correlation with the genotype, Orphanet J. Rare Dis. 6 (2011) 88. https://doi.org/10.1186/1750-1172-6-88.
[15] L. Folkestad, J.D. Hald, V. Canudas-Romo, J. Gram, A.P. Hermann, B. Langdahl, B. Abrahamsen, K. Brixen, Mortality and Causes of Death in Patients With Osteogenesis Imperfecta: A Register-Based Nationwide Cohort Study, J. Bone Miner. Res. 31 (2016) 2159–2166. https://doi.org/10.1002/jbmr.2895.
[16] J.R. Shapiro, P. Byers, F. Glorieux, P. Sponsellor, Osteogenesis Imperfecta: A Translational Approach to Brittle Bone Disease, Elsevier Inc., 2013. https://doi.org/10.1016/C2011-0-07790-6.
[17] S. Tournis, A.D. Dede, Osteogenesis imperfecta – A clinical update, Metab. - Clin. Exp. 80 (2018) 27–37. https://doi.org/10.1016/j.metabol.2017.06.001.
[18] A.L. Boskey, S.B. Doty, Chapter 4 - Mineralized Tissue: Histology, Biology and Biochemistry, in: J.R. Shapiro, P.H. Byers, F.H. Glorieux, P.D. Sponseller (Eds.), Osteogenes. Imperfecta, Academic Press, San Diego, 2014: pp. 31–43. https://doi.org/10.1016/B978-0-12-397165-4.00004-6.
[19] P. Fratzl, O. Paris, K. Klaushofer, W.J. Landis, Bone mineralization in an osteogenesis imperfecta mouse model studied by small-angle x-ray scattering., J. Clin. Invest. 97 (1996) 396–402.
[20] L. Imbert, J.-C. Aurégan, K. Pernelle, T. Hoc, Mechanical and mineral properties of osteogenesis imperfecta human bones at the tissue level, Bone. 65 (2014) 18–24. https://doi.org/10.1016/j.bone.2014.04.030.
[21] L. Imbert, J.-C. Aurégan, K. Pernelle, T. Hoc, Microstructure and compressive mechanical properties of cortical bone in children with osteogenesis imperfecta treated with bisphosphonates compared with healthy children, J. Mech. Behav. Biomed. Mater. 46 (2015) 261–270. https://doi.org/10.1016/j.jmbbm.2014.12.020.
[22] J.P. Cassella, P. Barber, A.C. Catterall, S.Y. Ali, A Morphometric analysis of osteoid collagen fibril diameter in osteogenesis imperfecta, Bone. 15 (1994) 329–334. https://doi.org/10.1016/8756-3282(94)90296-8.

[23] J. Becker, O. Semler, C. Gilissen, Y. Li, H.J. Bolz, C. Giunta, C. Bergmann, M. Rohrbach, F. Koerber, K. Zimmermann, P. de Vries, B. Wirth, E. Schoenau, B. Wollnik, J.A. Veltman, A. Hoischen, C. Netzer, Exome sequencing identifies truncating mutations in human SERPINF1 in autosomal-recessive osteogenesis imperfecta, Am. J. Hum. Genet. 88 (2011) 362–371. https://doi.org/10.1016/j.ajhg.2011.01.015.
[24] F.H. Glorieux, L.M. Ward, F. Rauch, L. Lalic, P.J. Roughley, R. Travers, Osteogenesis Imperfecta Type VI: A Form of Brittle Bone Disease with a Mineralization Defect, J. Bone Miner. Res. 17 (2002) 30–38. https://doi.org/10.1359/jbmr.2002.17.1.30.
[25] X. Bi, I. Grafe, H. Ding, R. Flores, E. Munivez, M.M. Jiang, B. Dawson, B. Lee, C.G. Ambrose, Correlations Between Bone Mechanical Properties and Bone Composition Parameters in Mouse Models of Dominant and Recessive Osteogenesis Imperfecta and the Response to Anti-TGF-β Treatment, J. Bone Miner. Res. 32 (2017) 347–359. https://doi.org/10.1002/jbmr.2997.
[26] I. Grafe, T. Yang, S. Alexander, E.P. Homan, C. Lietman, M.M. Jiang, T. Bertin, E. Munivez, Y. Chen, B. Dawson, Y. Ishikawa, M.A. Weis, T.K. Sampath, C. Ambrose, D. Eyre, H.P. Bächinger, B. Lee, Excessive transforming growth factor-β signaling is a common mechanism in osteogenesis imperfecta, Nat. Med. 20 (2014) 670–675. https://doi.org/10.1038/nm.3544.
[27] W.A. Cabral, W. Chang, A.M. Barnes, M. Weis, M.A. Scott, S. Leikin, E. Makareeva, N.V. Kuznetsova, K.N. Rosenbaum, C.J. Tifft, D.I. Bulas, C. Kozma, P.A. Smith, D.R. Eyre, J.C. Marini, Prolyl 3-hydroxylase 1 deficiency causes a recessive metabolic bone disorder resembling lethal/severe osteogenesis imperfecta, Nat. Genet. 39 (2007) 359–365. https://doi.org/10.1038/ng1968.
[28] N. Fratzl-Zelman, A.M. Barnes, M. Weis, E. Carter, T.E. Hefferan, G. Perino, W. Chang, P.A. Smith, P. Roschger, K. Klaushofer, F.H. Glorieux, D.R. Eyre, C. Raggio, F. Rauch, J.C. Marini, Non-Lethal Type VIII Osteogenesis Imperfecta Has Elevated Bone Matrix Mineralization, J. Clin. Endocrinol. Metab. 101 (2016) 3516–3525. https://doi.org/10.1210/jc.2016-1334.
[29] M.D. Shoulders, R.T. Raines, Collagen structure and stability, Annu. Rev. Biochem. 78 (2009) 929–958. https://doi.org/10.1146/annurev.biochem.77.032207.120833.
[30] B. Alexander, T.L. Daulton, G.M. Genin, J. Lipner, J.D. Pasteris, B. Wopenka, S. Thomopoulos, The nanometre-scale physiology of bone: steric modelling and scanning transmission electron microscopy of collagen–mineral structure, J. R. Soc. Interface. 9 (2012) 1774–1786. https://doi.org/10.1098/rsif.2011.0880.
[31] G.E. Fantner, T. Hassenkam, J.H. Kindt, J.C. Weaver, H. Birkedal, L. Pechenik, J.A. Cutroni, G.A.G. Cidade, G.D. Stucky, D.E. Morse, P.K. Hansma, Sacrificial bonds and hidden length dissipate energy as mineralized fibrils separate during bone fracture, Nat. Mater. 4 (2005) 612–616. https://doi.org/10.1038/nmat1428.
[32] M. Maghsoudi-Ganjeh, X. Wang, X. Zeng, Computational investigation of the effect of water on the nanomechanical behavior of bone, J. Mech. Behav. Biomed. Mater. 101 (2020) 103454. https://doi.org/10.1016/j.jmbbm.2019.103454.
[33] A.K. Nair, A. Gautieri, S.-W. Chang, M.J. Buehler, Molecular mechanics of mineralized collagen fibrils in bone, Nat. Commun. 4 (2013) 1724. https://doi.org/10.1038/ncomms2720.
[34] K. Beck, V.C. Chan, N. Shenoy, A. Kirkpatrick, J.A.M. Ramshaw, B. Brodsky, Destabilization of osteogenesis imperfecta collagen-like model peptides correlates with the identity of the residue replacing glycine, Proc. Natl. Acad. Sci. 97 (2000) 4273–4278. https://doi.org/10.1073/pnas.070050097.
[35] J.C. Marini, A. Forlino, W.A. Cabral, A.M. Barnes, J.D.S. Antonio, S. Milgrom, J.C. Hyland, J. Körkkö, D.J. Prockop, A.D. Paepe, P. Coucke, S. Symoens, F.H. Glorieux, P.J. Roughley, A.M. Lund, K. Kuurila-Svahn, H. Hartikka, D.H. Cohn, D. Krakow, M. Mottes, U. Schwarze, D. Chen, K. Yang, C. Kuslich, J. Troendle, R. Dalgleish, P.H. Byers, Consortium for osteogenesis imperfecta mutations in the helical domain of type I collagen: regions rich in lethal mutations align with collagen binding sites for integrins and proteoglycans, Hum. Mutat. 28 (2007) 209–221. https://doi.org/10.1002/humu.20429.

[36] S.-W. Chang, S.J. Shefelbine, M.J. Buehler, Structural and Mechanical Differences between Collagen Homo- and Heterotrimers: Relevance for the Molecular Origin of Brittle Bone Disease, Biophys. J. 102 (2012) 640–648. https://doi.org/10.1016/j.bpj.2011.11.3999.
[37] A. Gautieri, S. Uzel, S. Vesentini, A. Redaelli, M.J. Buehler, Molecular and Mesoscale Mechanisms of Osteogenesis Imperfecta Disease in Collagen Fibrils, Biophys. J. 97 (2009) 857–865. https://doi.org/10.1016/j.bpj.2009.04.059.
[38] A. Gautieri, S. Vesentini, A. Redaelli, M.J. Buehler, Single molecule effects of osteogenesis imperfecta mutations in tropocollagen protein domains, Protein Sci. Publ. Protein Soc. 18 (2009) 161–168. https://doi.org/10.1002/pro.21.
[39] A. Gautieri, S. Vesentini, A. Redaelli, M.J. Buehler, Osteogenesis imperfecta mutations lead to local tropocollagen unfolding and disruption of H-bond network, RSC Adv. 2 (2012) 3890–3896. https://doi.org/10.1039/C2RA01047J.
[40] J. Yeo, G. Jung, A. Tarakanova, F.J. Martín-Martínez, Z. Qin, Y. Cheng, Y.-W. Zhang, M.J. Buehler, Multiscale modeling of keratin, collagen, elastin and related human diseases: Perspectives from atomistic to coarse-grained molecular dynamics simulations, Extreme Mech. Lett. 20 (2018) 112–124. https://doi.org/10.1016/j.eml.2018.01.009.
[41] A. Ghanaeian, R. Soheilifard, Mechanical elasticity of proline-rich and hydroxyproline-rich collagen-like triple-helices studied using steered molecular dynamics, J. Mech. Behav. Biomed. Mater. 86 (2018) 105–112. https://doi.org/10.1016/j.jmbbm.2018.06.021.
[42] M. Unal, S. Uppuganti, C.J. Leverant, A. Creecy, M. Granke, P. Voziyan, J.S. Nyman, Assessing glycation-mediated changes in human cortical bone with Raman spectroscopy, J. Biophotonics. 11 (2018) e201700352. https://doi.org/10.1002/jbio.201700352.
[43] C. Olejnik, G. Falgayrac, A. During, B. Cortet, G. Penel, Doses effects of zoledronic acid on mineral apatite and collagen quality of newly-formed bone in the rat's calvaria defect, Bone. 89 (2016) 32–39. https://doi.org/10.1016/j.bone.2016.05.002.
[44] N.A. Lygidakis, R. Smith, C.J. Oulis, Scanning electron microscopy of teeth in osteogenesis imperfecta type I, Oral Surg. Oral Med. Oral Pathol. Oral Radiol. Endod. 81 (1996) 567–572. https://doi.org/10.1016/S1079-2104(96)80048-5.
[45] S. Opsahl Vital, C. Gaucher, C. Bardet, P.S. Rowe, A. George, A. Linglart, C. Chaussain, Tooth dentin defects reflect genetic disorders affecting bone mineralization, Bone. 50 (2012) 989–997. https://doi.org/10.1016/j.bone.2012.01.010.
[46] W.T. Butler, J.C. Brunn, C. Qin, Dentin extracellular matrix (ECM) proteins: comparison to bone ECM and contribution to dynamics of dentinogenesis, Connect. Tissue Res. 44 Suppl 1 (2003) 171–178.
[47] S. Pragnère, C. Boulocher, O. Pollet, C. Bosser, A. Levillain, M. Cruel, T. Hoc, Mechanical alterations of the bone-cartilage unit in a rabbit model of early osteoarthrosis, J. Mech. Behav. Biomed. Mater. 83 (2018) 1–8. https://doi.org/10.1016/j.jmbbm.2018.03.033.
[48] W.C. Oliver, G.M. Pharr, An improved technique for determining hardness and elastic modulus using load and displacement sensing indentation experiments, J. Mater. Res. 7 (1992) 1564–1583. https://doi.org/10.1557/JMR.1992.1564.
[49] J.H. Kinney, M. Balooch, S.J. Marshall, G.W. Marshall, T.P. Weihs, Hardness and Young's modulus of human peritubular and intertubular dentine, Arch. Oral Biol. 41 (1996) 9–13. https://doi.org/10.1016/0003-9969(95)00109-3.
[50] D. Ziskind, M. Hasday, S.R. Cohen, H.D. Wagner, Young's modulus of peritubular and intertubular human dentin by nano-indentation tests, J. Struct. Biol. 174 (2011) 23–30. https://doi.org/10.1016/j.jsb.2010.09.010.
[51] C. Bosser, A. Ogier, L. Imbert, T. Hoc, Raman Spectroscopy as a Biomarker-Investigative Tool in Bone Metabolism, in: V.R. Preedy (Ed.), Biomark. Bone Dis., Springer Netherlands, 2016: pp. 1–27. https://doi.org/10.1007/978-94-007-7745-3_31-1.
[52] K. Chatzipanagis, C.G. Baumann, M. Sandri, S. Sprio, A. Tampieri, R. Kröger, In situ mechanical and molecular investigations of collagen/apatite biomimetic composites combining Raman

spectroscopy and stress-strain analysis, Acta Biomater. 46 (2016) 278–285. https://doi.org/10.1016/j.actbio.2016.09.028.
[53] J.S. Yerramshetty, O. Akkus, The associations between mineral crystallinity and the mechanical properties of human cortical bone, Bone. 42 (2008) 476–482. https://doi.org/10.1016/j.bone.2007.12.001.
[54] J.H. Kinney, S. Habelitz, S.J. Marshall, G.W. Marshall, The importance of intrafibrillar mineralization of collagen on the mechanical properties of dentin, J. Dent. Res. 82 (2003) 957–961. https://doi.org/10.1177/154405910308201204.
[55] J.H. Kinney, S.J. Marshall, G.W. Marshall, The mechanical properties of human dentin: a critical review and re-evaluation of the dental literature, Crit. Rev. Oral Biol. Med. Off. Publ. Am. Assoc. Oral Biol. 14 (2003) 13–29. https://doi.org/10.1177/154411130301400103.
[56] C. Montoya, S. Arango-Santander, A. Peláez-Vargas, D. Arola, E.A. Ossa, Effect of aging on the microstructure, hardness and chemical composition of dentin, Arch. Oral Biol. 60 (2015) 1811–1820. https://doi.org/10.1016/j.archoralbio.2015.10.002.
[57] Y.-R. Zhang, W. Du, X.-D. Zhou, H.-Y. Yu, Review of research on the mechanical properties of the human tooth, Int. J. Oral Sci. 6 (2014) 61–69. https://doi.org/10.1038/ijos.2014.21.
[58] A. Slimani, F. Nouioua, A. Desoutter, B. Levallois, F.J.G. Cuisinier, H. Tassery, E. Terrer, H. Salehi, Confocal Raman mapping of collagen cross-link and crystallinity of human dentin–enamel junction, J. Biomed. Opt. 22 (2017) 086003. https://doi.org/10.1117/1.JBO.22.8.086003.
[59] W. Tesch, N. Eidelman, P. Roschger, F. Goldenberg, K. Klaushofer, P. Fratzl, Graded Microstructure and Mechanical Properties of Human Crown Dentin, Calcif. Tissue Int. 69 (2001) 147–157. https://doi.org/10.1007/s00223-001-2012-z.
[60] R.Z. Wang, S. Weiner, Strain-structure relations in human teeth using Moiré fringes, J. Biomech. 31 (1998) 135–141. https://doi.org/10.1016/s0021-9290(97)00131-0.
[61] G.R. Davis, J.M. Fearne, N. Sabel, J.G. Norén, Microscopic study of dental hard tissues in primary teeth with Dentinogenesis Imperfecta Type II: Correlation of 3D imaging using X-ray microtomography and polarising microscopy, Arch. Oral Biol. 60 (2015) 1013–1020. https://doi.org/10.1016/j.archoralbio.2015.03.010.
[62] A. Wieczorek, J. Loster, W. Ryniewicz, A.M. Ryniewicz, Dentinogenesis imperfecta - hardness and Young's modulus of teeth, Acta Bioeng. Biomech. 15 (2013) 65–69.
[63] G.E. Lopez Franco, A. Huang, N. Pleshko Camacho, D.S. Stone, R.D. Blank, Increased Young's Modulus and Hardness of Col1a2oim Dentin, J. Dent. Res. 85 (2006) 1032–1036.
[64] G.S. Mandair, M.D. Morris, Contributions of Raman spectroscopy to the understanding of bone strength, BoneKEy Rep. 4 (2015) 620. https://doi.org/10.1038/bonekey.2014.115.
[65] M.D. Morris, G.S. Mandair, Raman Assessment of Bone Quality, Clin. Orthop. Relat. Res. 469 (2011) 2160–2169. https://doi.org/10.1007/s11999-010-1692-y.
[66] E.P. Paschalis, S. Gamsjaeger, K. Klaushofer, Vibrational spectroscopic techniques to assess bone quality, Osteoporos. Int. 28 (2017) 2275–2291. https://doi.org/10.1007/s00198-017-4019-y.
[67] X. Bi, C.A. Patil, C.C. Lynch, G.M. Pharr, A. Mahadevan-Jansen, J.S. Nyman, Raman and mechanical properties correlate at whole bone- and tissue-levels in a genetic mouse model, J. Biomech. 44 (2011) 297–303. https://doi.org/10.1016/j.jbiomech.2010.10.009.
[68] N. Reznikov, M. Bilton, L. Lari, M.M. Stevens, R. Kröger, Fractal-like hierarchical organization of bone begins at the nanoscale, Science. 360 (2018). https://doi.org/10.1126/science.aao2189.
[69] M.J. Buehler, Nature designs tough collagen: Explaining the nanostructure of collagen fibrils, Proc. Natl. Acad. Sci. 103 (2006) 12285–12290. https://doi.org/10.1073/pnas.0603216103.
[70] G.K. Toworfe, R.J. Composto, I.M. Shapiro, P. Ducheyne, Nucleation and growth of calcium phosphate on amine-, carboxyl- and hydroxyl-silane self-assembled monolayers, Biomaterials. 27 (2006) 631–642. https://doi.org/10.1016/j.biomaterials.2005.06.017.
[71] K. Buckley, P. Matousek, A.W. Parker, A.E. Goodship, Raman spectroscopy reveals differences in collagen secondary structure which relate to the levels of mineralisation in bones that have

evolved for different functions, J. Raman Spectrosc. 43 (2012) 1237–1243. https://doi.org/10.1002/jrs.4038.
[72] N. Almora-Barrios, K.F. Austen, N.H. de Leeuw, Density Functional Theory Study of the Binding of Glycine, Proline, and Hydroxyproline to the Hydroxyapatite (0001) and (01$\bar{1}$0) Surfaces, Langmuir. 25 (2009) 5018–5025. https://doi.org/10.1021/la803842g.
[73] M. Gąsior-Głogowska, M. Komorowska, J. Hanuza, M. Ptak, M. Kobielarz, Structural alteration of collagen fibres--spectroscopic and mechanical studies, Acta Bioeng. Biomech. 12 (2010) 55–62.
[74] Y.-N. Wang, C. Galiotis, D.L. Bader, Determination of molecular changes in soft tissues under strain using laser Raman microscopy, J. Biomech. 33 (2000) 483–486. https://doi.org/10.1016/S0021-9290(99)00194-3.

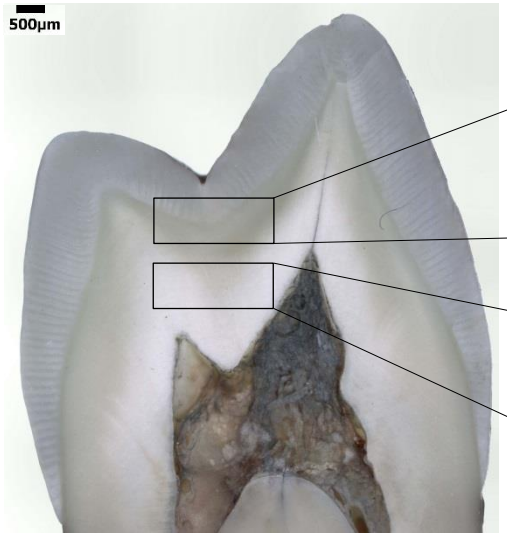
500µm

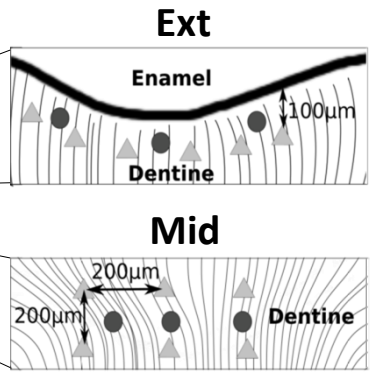
Ext
Enamel
100µm
Dentine
Mid
200µm
200µm
Dentine
Raman spot
Indent location

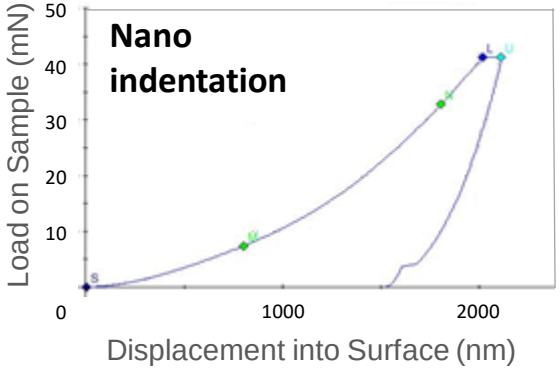
Nano indentation
Load on Sample (mN)
Displacement into Surface (nm)

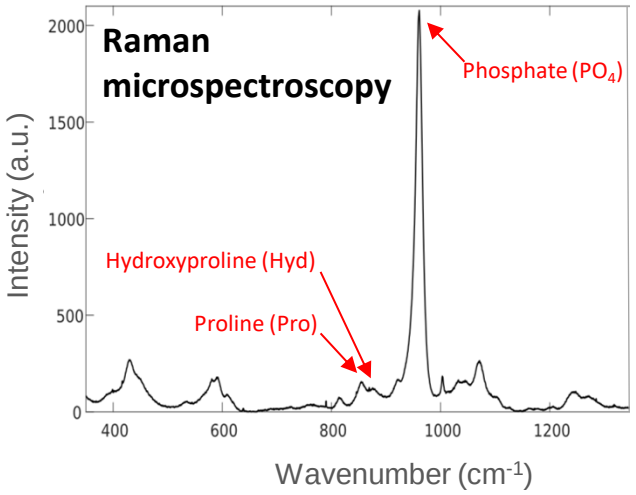
Raman microspectroscopy
Phosphate (PO4)
Hydroxyproline (Hyd)
Proline (Pro)
Intensity (a.u.)
Wavenumber (cm-1)

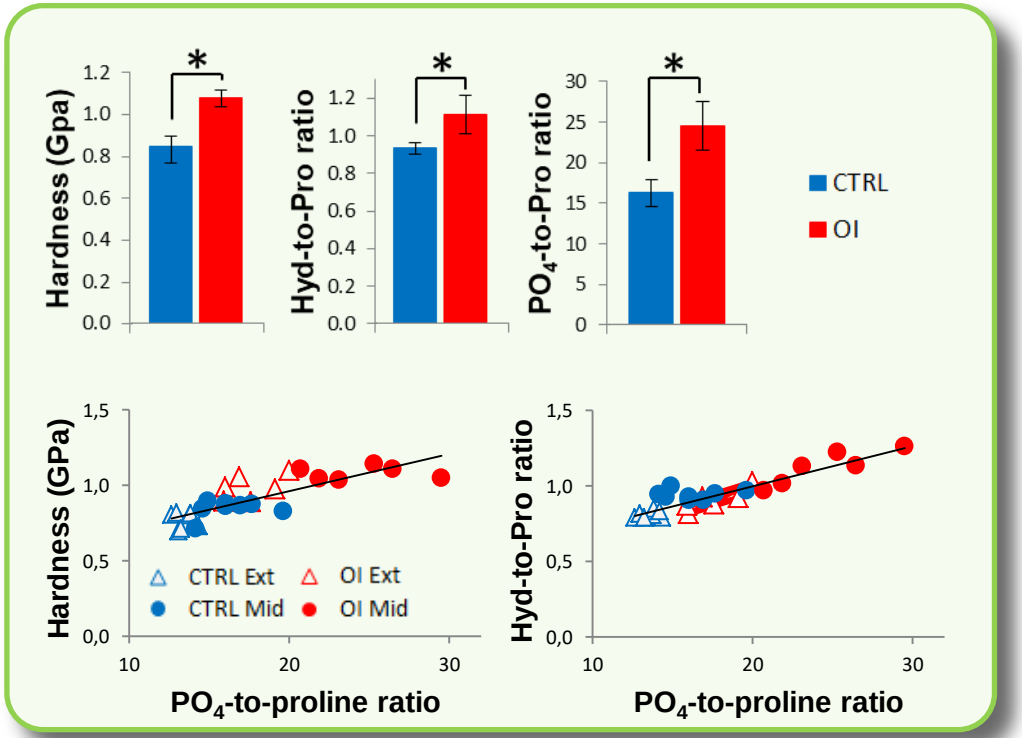
Hardness (Gpa)
Hyd-to-Pro ratio
PO4-to-Pro ratio
CTRL
OI
Hardness (GPa)
CTRL Ext
OI Ext
CTRL Mid
OI Mid
PO4-to-proline ratio
Hyd-to-Pro ratio
PO4-to-proline ratio